J Physiol 586.22 (2008) pp 5403–5418

The Journal of Physiology

TRPML3 mutations cause impaired mechano-electrical transduction and depolarization by an inward-rectifier cation current in auditory hair cells of varitint-waddler mice

Alexander F. J. van Aken[1], Margaret Atiba-Davies[2], Walter Marcotti[1], Richard J. Goodyear[1], Jane E. Bryant[1], Guy P. Richardson[1], Konrad Noben-Trauth[2] and Corné J. Kros[1]

[1]*School of Life Sciences, University of Sussex, Falmer, Brighton BN1 9QG, UK*
[2]*National Institute on Deafness and Other Communication Disorders, National Institutes of Health, 5 Research Court, Rockville, MD 20850, USA*

TRPML3 (mucolipin-3) belongs to one of the transient-receptor-potential (TRP) ion channel families. Mutations in the *Trpml3* gene cause disorganization of the stereociliary hair bundle, structural aberrations in outer and inner hair cells and stria vascularis defects, leading to deafness in the varitint-waddler (*Va*) mouse. Here we refined the stereociliary localization of TRPML3 and investigated cochlear hair cell function in varitint-waddler (Va^J) mice carrying the TRPML3<I362T/A419P> mutations. Using a TRPML3-specific antibody we detected a ∼68 kDa protein with near-equal expression levels in cochlea and vestibule of wild-type and Va^J mutants. At postnatal days 3 and 5, we observed abundant localization of TRPML3 at the base of stereocilia near the position of the ankle links. This stereociliary localization domain was absent in Va^J heterozygotes and homozygotes. Electrophysiological recordings revealed reduced mechano-electrical transducer currents in hair cells from $Va^J/+$ and Va^J/Va^J mice. Furthermore, FM1-43 uptake and [^{3}H]gentamicin accumulation were decreased in hair cells in cultured organs of Corti from $Va^J/+$ and Va^J/Va^J mice. We propose that TRPML3 plays a critical role at the ankle-link region during hair-bundle growth and that an adverse effect of mutant TRPML3 on bundle development and mechano-electrical transduction is the main cause of hearing loss in $Va^J/+$ mutant mice. Outer hair cells of Va^J/Va^J mice additionally had depolarized resting potentials due to an inwardly rectifying leak conductance formed by the mutant channels, leading over time to hair-cell degeneration and contributing to their deafness. Our findings argue against TRPML3 being a component of the hair-cell transducer channel.

(Resubmitted 16 May 2008; accepted after revision 16 September 2008; first published online 18 September 2008)
Corresponding authors C. J. Kros: School of Life Sciences, University of Sussex, Falmer, Brighton BN1 9QG, UK. Email: c.j.kros@sussex.ac.uk; K. Noben-Trauth: National Institute on Deafness and Other Communication Disorders, National Institutes of Health, 5 Research Court, Rockville, MD 20850, USA. Email: nobentk@nidcd.nih.gov

In the mammalian cochlea, inner and outer hair cells (IHCs and OHCs) function as primary transducers of acoustic stimuli. Nanometer displacements of the hair bundle open mechanosensitive transducer channels located near the tips of the stereocilia (Denk *et al.* 1995; Lumpkin & Hudspeth, 1995; Geleoc *et al.* 1997). The resulting influx of K^+ and Ca^{2+} generates the receptor potential, converting the mechanical stimuli into electrical signals. Although a number of candidates, including members of some of the transient receptor potential (TRP) channel families (Clapham, 2003; Pedersen *et al.* 2005), have been proposed, the proteins that form the transducer channel complex of the mammalian hair cell are unknown (Corey, 2006; Ricci *et al.* 2006; Cuajungco *et al.* 2007).

The varitint-waddler mouse exhibits deafness, circling behaviour and pigmentation abnormalities resulting from two spontaneous mutations, *Va* and Va^J, in the *Trpml3* gene (also named *Mcoln3*) (Cloudman & Bunker, 1945; Di Palma *et al.* 2002). *Va* and Va^J mice have congenital hearing loss and show structural defects in the stria vascularis and cochlear hair cells, ultimately leading to degeneration of the stria and organ of Corti (Deol, 1954; Cable & Steel, 1998; Kim *et al.* 2002). Stereociliary splaying in *Va* and Va^J mutants starts around day 17.5 of gestation (E17.5), 2 days before birth, and progressively worsens

DOI: 10.1113/jphysiol.2008.156992

during the first postnatal days. The onset of the pathology coincides approximately with the differentiation of the hair bundle (Goodyear *et al.* 2005) and the establishment of its mechanosensitive properties (Bryant *et al.* 2003; Waguespack *et al.* 2007). This has led to TRMPL3 being discussed as a candidate for the mammalian transducer channel or one of its subunits (Beurg *et al.* 2006; Corey, 2006).

TRPML3 encodes a 553 amino acid protein with a predicted molecular weight of ∼68 kDa that has the transient receptor potential (TRP) cation channel motif (PS50272) characteristic for many TRP channels (Qian & Noben-Trauth, 2005; Atiba-Davies & Noben-Trauth, 2007). The *Va* allele encodes a missense mutation (Ala419Pro), which is located near the predicted pore region in the fifth transmembrane domain. The A419P substitution is a semidominant allele and is thought to act as a gain-of-function mutation (Grimm *et al.* 2007; Kim *et al.* 2007; Xu *et al.* 2007). In the Va^J allele, the Ile362Thr missense mutation occurred in *cis* to the A419P substitution, in the second extracellular loop, and appears to have an attenuating effect on the Va^J phenotype. Recent molecular studies showed that *in vitro*-expressed wild-type TRPML3 acts as an inwardly rectifying cation channel that is gated, in a complex manner, by extracellular Na^+ levels and pH, whereas the mutant TRPML3< A419P> isoform forms a constitutively open channel (Grimm *et al.* 2007; Kim *et al.* 2007, 2008; Xu *et al.* 2007). As expected from the attenuated phenotype of Va^J mice, the I362T mutation, when placed in the context of the A419P mutation (TRPML3<I362T/A419P>) diminishes current density and reduces expression of the protein on the cell surface (Grimm *et al.* 2007; Kim *et al.* 2007). Initial immunostaining on cochlear hair cells localized TRPML3 to vesicles in the hair cell cytoplasm and to the plasma membrane of stereocilia (Di Palma *et al.* 2002). The present work was conducted to refine the stereociliary localization of TRPML3 and to ascertain whether varitint-waddler mutations had any consequences for mechano-electrical transduction by cochlear hair cells.

Methods

Mice

C3HeB/FeJ mice were obtained from The Jackson Laboratory (Bar Harbour, ME, USA). The Va^J (B6C3Fe-a/a Hoxa13Hd Mcoln3Va-J/J; stock number 00296) allele was initially obtained from The Jackson Laboratory and subsequently made congenic to the C3HeB/FeJ strain (available through MMRRC stock 11149). Animal care and use were in accordance with guidelines at NIH (USA) and the Home Office (UK). Mice were killed by cervical dislocation before dissection of cochlear tissues.

Immunofluorescence

TRPML3 was detected with affinity-purified polyclonal HL4460 antiserum directed against a peptide epitope located downstream of the sixth transmembrane domain (amino acids (AAs) 529–548) and with affinity-purified polyclonal PB221 antiserum directed against a peptide epitope located at the third extracellular loop (AAs 446–462) (Di Palma *et al.* 2002). Cochleae were dissected in Leibovitz medium (Invitrogen) and fixed in 4% paraformaldehyde (Electron Microscopy Sciences) in phosphate-buffered saline (PBS) for 2 h at room temperature. The tectorial membrane was removed and the tissue was permeabilized with 0.5% Triton X-100 in PBS for 30 min. The tissue was then washed three times in PBS for 10 min each and blocked with 5% goat serum, 2% BSA in PBS at 4°C overnight. Samples were washed three times and incubated in affinity-purified antibody HL4460 or PB221 (1 : 1000 in blocking solution) for 2 h at room temperature, washed in PBS, and incubated with secondary anti-rabbit IgG (Alexa Fluor 594 donkey, Invitrogen) for 1 h at room temperature. The specimens were washed and counterstained with Alexa Fluor 488 phalloidin (Invitrogen), diluted 1 : 100 in PBS for 1 h at room temperature. After washing with PBS, the organ of Corti was dissected, mounted in ProLong Gold antifade reagent (Invitrogen), and imaged using a Zeiss LSM confocal microscope.

Immunogold labelling

Cochlear cultures were prepared from P2 C57BL6J mice on collagen-coated glass coverslips as previously described (Russell & Richardson, 1987) and maintained in Maximow slide assemblies for 2 days at 37°C in a medium containing 93% DMEM/F12, 7% fetal bovine serum and 10 μg ml^{-1} ampicillin. Following a brief rinse in Hepes-buffered Hanks' balanced salt solution (HBHBSS), cultures were fixed for 1 h in 4% paraformaldehyde/0.1 M sodium phosphate buffer, washed in PBS, preblocked in TBS/10% goat serum, and stained overnight at 4°C with affinity-purified PB221 (1 : 500 dilution) or, as a control, non-immune rabbit IgG (2 μg ml^{-1}). After five washes in PBS, cultures were labelled overnight with 5 nm colloidal gold-conjugated goat anti-rabbit IgG diluted 1 : 10 in PBS/10% goat serum, washed, refixed with 2.5% glutaraldehyde followed by 1% osmium tetroxide (both in 0.1 M sodium cacodylate buffer pH 7.2 containing 0.5% ruthenium red), dehydrated with ethanol, and embedded in Epoxy resin. Sections were cut at ∼100 nm thickness, mounted on copper grids, double stained with uranyl

acetate and lead citrate and viewed in a Hitachi 7100 transmission electron microscope equipped with a Gatan Ultrascan 1000 CCD camera.

TRPML3 expression construct and transfection

Wild-type *Trpml3* cDNA was amplified by PCR using C57BL/6J cochlear cDNA with primers 5′-CCTGAA-TTCACCAGAGATGGCAAATCCCGAG-3′ (forward) and 5′-TGGATCCCTTTTTGCAGCAGCAGAGTAAAGA-3′ (reverse) flanked by *Eco*R I and *Bam*H I restriction sites. The 1682 bp *Trpml3* PCR product was cloned into pcDNA 3.1/CT-GFP-TOPO vector (Invitrogen).

COS-1 cells (African green monkey kidney cell line, ATCC) were cultured in Dulbecco's modified Eagle's medium (Gibco), supplemented with 10% fetal bovine serum (Gemini Biosciences), 100 U ml^{-1} penicillin and 100 $\mu g\,ml^{-1}$ streptomycin (Gibco, Invitrogen Life Technologies) at 37°C with 5% CO_2 in a humidified incubator. For transient transfections cells were grown to 30% confluency and transfected with GeneJuice transfection reagent (Novagen) at a ratio of 3 : 1 GeneJuice : DNA according to the manufacturer's instructions. For immunofluorescence, cells were seeded directly onto sterile glass coverslips and transfections were carried out as above. Transfected cells were examined 48 h following transfection. Cells were treated with 4% paraformaldehyde, then permeabilized with 0.5% Triton X-100 for 10 min each. Non-specific binding sites were blocked in blocking solution (PBS, 2% BSA, 0.1% Triton X-100), for 1 h and then coverslips were incubated for 1 h with HL4460 antibody diluted in blocking buffer. Coverslips were washed with PBS, then incubated for 1 h with labelled secondary antibody (Alexa 594 goat anti-rabbit, Molecular Probes). Coverslips were washed as before, then mounted in Vectashield (Vector Laboratories) onto glass microscopic slides and examined with a laser scanning confocal microscope (LSM 510, Zeiss).

Western blot analysis

Transfected cells were either harvested and homogenized in a lysis buffer that contained 50 mM Tris-HCl pH 7.4, 150 mM NaCl, 1% NP-40, 0.5% NaDOC, 0.1% SDS and protease inhibitors (complete protease inhibitor cocktail tablets, Roche Applied Science) or lysed directly into Laemmli buffer containing 8 M urea and 300 mM DTT. Protein concentrations were determined by RC DC protein assay (Bio-Rad). Cell lysates (25 μg) were subjected to 8 M urea/SDS 8% (v/v) polyacrylamide gel electrophoresis. For cochlear and vestibular extracts inner ear tissues were harvested from mice at postnatal day (P)21 followed by homogenization in lysis buffer (as above). Proteins were solubilized for 1 h on ice and then centrifuged at 20 000 r.c.f. for 30 min at 4°C. Extracts were concentrated with a YM10 Microcon filter (Millipore) and the protein concentration was determined prior to gel electrophoresis on a NuPAGE 4–20% Bis-Tris gel system (Invitrogen). Proteins were blotted onto PVDF membrane (Bio-Rad). Membranes were subsequently blocked with 5% non-fat dry milk, 0.1% Tween-20 in Tris-buffered saline, overnight at 4°C. TRPML3 was detected with affinity-purified polyclonal HL4460 anti-serum. Anti-green fluorescent protein (GFP)-antibody was obtained from Invitrogen. Secondary antibody was goat anti-rabbit alkaline phosphatase (Bio-Rad) and proteins were visualized with the Immune Star chemiluminescence protein detection system (Bio-Rad).

Hair-cell electrophysiology

OHCs from varitint-waddler mutant (Va^J/Va^J, $Va^J/+$) and matching congenic control (+/+) mice were studied either in organotypic cochlear cultures (age P1) plus 2 days *in vitro* in sealed Maximow slide assemblies at 37°C) (Russell & Richardson, 1987), or, for the vast majority of experiments, following acute dissection of the organ of Corti (P0–P6). After acute dissection, organs of Corti were transferred to a recording chamber in which they were immobilized under a nylon mesh fixed to a stainless steel ring. The position along the cochlea, as fractional distance from the extreme apex, was about 0.15–0.25 for apical coil OHCs and 0.65–0.85 for basal coil OHCs. All experiments were conducted at room temperature (22–27°C). Extracellular solution was continuously bath-applied and contained (in mM): 135 NaCl, 5.8 KCl, 1.3 $CaCl_2$, 0.9 $MgCl_2$, 0.7 NaH_2PO_4, 2 sodium pyruvate, 5.6 D-glucose, and 10 Hepes. Amino acids and vitamins for Eagle's minimum essential medium (MEM) were added from concentrates (Invitrogen). The pH was adjusted to 7.5 and the osmolality was about 308 mosmol kg^{-1}. For some experiments, the transducer channel blockers neomycin (Sigma) and FM1-43 (n-(3-triethylammoniumpropyl)-4-(4-(dibutylamino) styryl)pyridiniumdibromide (Invitrogen) were added to the extracellular solution and bath-perfused over acutely dissected organs of Corti for between 5 and 30 min. This ensures access to and, if applicable, block of ion channels on both the apical and basolateral surfaces of the hair cells.

Mechano-electrical transducer currents were elicited in OHCs using fluid-jet stimulation (45 Hz sine waves filtered at 1 kHz, 8-pole Bessel) and recorded under whole-cell voltage clamp with Optopatch (Cairn Research, Faversham, UK) or EPC8 (HEKA, Lambrecht, Germany) patch clamp amplifiers as previously described (Kros *et al.* 1992, 1993). For consistency between recordings, the amplitude of the driver voltage to the fluid jet was

fixed at 35 V unless otherwise indicated, which elicits large, near-saturating transducer currents in control cells. Plots of transducer currents as a function of driver voltage during the sinusoidal stimuli were constructed, with a correction for a presumed 800 μs delay between driver voltage and bundle movement (Kros *et al.* 1993). Patch pipettes (resistance in the bath 2–3 MΩ) were pulled from soda glass capillaries and coated with wax. Intracellular solutions contained (in mM): 137 CsCl, 10 sodium phosphocreatine, 2.5 $MgCl_2$, 1 EGTA-CsOH, 2.5 Na_2ATP, 5 Hepes (for some cells no sodium phosphocreatine was present and the CsCl concentration was increased to 147 mM, with no obvious effects on the membrane currents) or 131 KCl, 10 sodium phosphocreatine, 3 $MgCl_2$, 1 EGTA-KOH, 5 Na_2ATP, 5 Hepes; pH adjusted to 7.3 with 1 M CsOH or KOH, respectively. The osmolality was about 295 mosmol kg^{-1}. Data were low-pass filtered at 2.5–3.0 kHz and sampled at 5 kHz using a Power 1401 data acquisition interface and Signal 3 software (CED, Cambridge, UK).

Membrane potentials were corrected for a −4 mV liquid junction potential between pipette and bath solutions. Residual series resistance (R_s) after compensation was 1.89 ± 0.22 MΩ ($n = 68$). For experiments with K^+-based intracellular solutions membrane potentials were corrected for the voltage drop across R_s. No such corrections were applied to the recordings in which basolateral K^+ currents were minimized with Cs^+-based intracellular solutions, as maximum voltage drops were below 5 mV. Voltage-clamp protocols are in reference to a holding potential of −84 mV.

Statistical comparisons of means were made using analysis of variance (one-way ANOVA followed by Tukey's post test) and $P < 0.05$ was used as the criterion for statistical significance. Mean values are quoted ± S.E.M. in text and figures.

FM1–43 labelling

Cochlear cultures were prepared from varitint-waddler mutant (*Va*^{J}/*Va*^{J} and *Va*^{J}/+) and congenic control (+/+) mice and maintained at 37°C for 2 days. Stock solutions of 3 mM FM1-43 were dissolved in either DMSO or water. FM1-43 dye labelling was studied after bath application. The coverslips, with adherent organotypic cultures, were removed from the Maximow slide assemblies and transferred through a series of Columbia staining jars, each containing 8 ml of solution. All experiments were performed at room temperature. The coverslips were immersed in HBHBSS for 15 min, transferred to HBHBSS containing 3 μM FM1-43 for 10 s, and then immediately washed three times (10 s for each wash) in HBHBSS (Gale *et al.* 2001). The coverslips were then placed in a glass-bottomed Perspex chamber containing 1.5 ml HBHBSS and viewed with an upright microscope equipped with epifluorescence optics and FITC filters (excitation 488 nm, emission 520 nm) using a ×63 water immersion objective. Images were captured from live cultures at fixed time points after dye application using a 12-bit cooled CCD camera (SPOT-JNR). The number of cochlear cultures used, each of which contained two apical and two basal coil explants, was: 6 (+/+), 8 (*Va*^{J}/+) and 3 (*Va*^{J}/*Va*^{J}).

[^{3}H]Gentamicin labelling

Coverslips with adherent cochlear cultures were removed from Maximow slide assemblies, placed in 35 mm diameter plastic culture dishes, washed 3 × with HBHBSS, and incubated in HBHBSS containing 0.1 mM [^{3}H]gentamicin (Amersham, UK) for 2 h at 37°C. Cultures were then placed on ice, washed 3 × with 4 ml of ice-cold HBHBSS over a 10 min period, and fixed in cold 2.5% glutaraldehyde buffered with 0.1 M sodium cacodylate, pH 7.2 for 1 h. Following fixation in 2.5% glutaraldehyde, the cultures were washed 3 × in 0.1 M cacodylate buffer, fixed for 1 h with 1% osmium tetroxide, washed in buffer, dehydrated through a series of ascending concentrations of ethanol and embedded in Epon 812 resin (TAAB, Berks, UK). Sections, 1 μm thick, of the apical and basal cochlear coils were cut from the cured plastic blocks with glass knives, mounted on glass slides and either stained with toluidine blue or coated with Ilford L4 Nuclear Research Emulsion (Ilford Imaging UK Limited, Mobberley, UK) for autoradiography. Emulsion-coated slides were exposed in light-tight boxes in the presence of drying agent at 4°C for 1–3 weeks, and developed in Ilford Phenisol (diluted 1 + 4 with H_2O) for 4 min at 18°C. Developed autoradiographs were washed, fixed and dried, mounted under glass coverslips using a drop of Histomount, and viewed with an Axioplan 2 light microscope using phase contrast optics.

Results

TRPML3 is expressed in the inner ear of wild-type and *Va*^{J} mutant mice

The affinity-purified HL4460 polyclonal antiserum was raised against an intracellular carboxyterminal epitope of mouse TRPML3. To determine its specificity, we constructed a TRPML3-GFP fusion protein using a *Trpml3* cDNA transcribed from mouse cochlear mRNA. In protein extracts of transiently transfected COS cells the HL4460 antibody detected a band of approximately 91 kDa (Fig. 1*A*, arrowhead) corresponding to the expected molecular mass for GFP-tagged TRPML3, and a slower migrating doublet of approximately 215 kDa (Fig. 1*A*,

arrow). In the same extracts, an antibody against the GFP moiety recognized both the 91 kDa and the 215 kDa bands (Fig. 1*A*), thus correlating with the bands detected using HL4460. No endogenous TRPML3 protein was detected in extracts from cells that had not been transfected or transfected with vector alone. While the 91 kDa product corresponds to the calculated molecular weight for a full-length TRPML3-GFP fusion protein, the larger products at ∼215 kDa may represent TRPML3 dimers or heterodimeric complexes. Interaction of TRPML molecules in homomeric and heteromeric combinations (Venkatachalam *et al.* 2006) and the formation of larger molecular weight species of the Myc-tagged TRPML1 (Manzoni *et al.* 2004) *in vitro* systems have been observed.

To test the specificity and sensitivity of HL4460 under native conditions we probed protein extracts from inner ear organs of wild-type and varitint-waddler mutants. In cochlear and vestibular tissue from wild-type (+/+), heterozygous (Va^J/+) and homozygous (Va^J/Va^J) mice HL4460 antibody detected a single product of ∼68 kDa (Fig. 1*B*, arrowhead). The level of TRPML3 protein was similar in vestibule and cochlea and across the genotypes. COS cells expressing the TRPML3-GFP fusion protein were also immunostained with HL4460. We observed a perfect co-localization of the GFP domain with the HL4460 epitope (Fig. 1*C*).

TRPML3 localizes to the base of cochlear hair-cell stereocilia

Abnormalities of the hair bundles often result from mutations in proteins that are targeted to stereocilia where they play important structural and functional roles. The stereociliary defects in varitint-waddler hair cells argued that TRPML3 might have a corresponding localization. To refine our previous localization, we performed immuno-labelling of organ of Corti surface

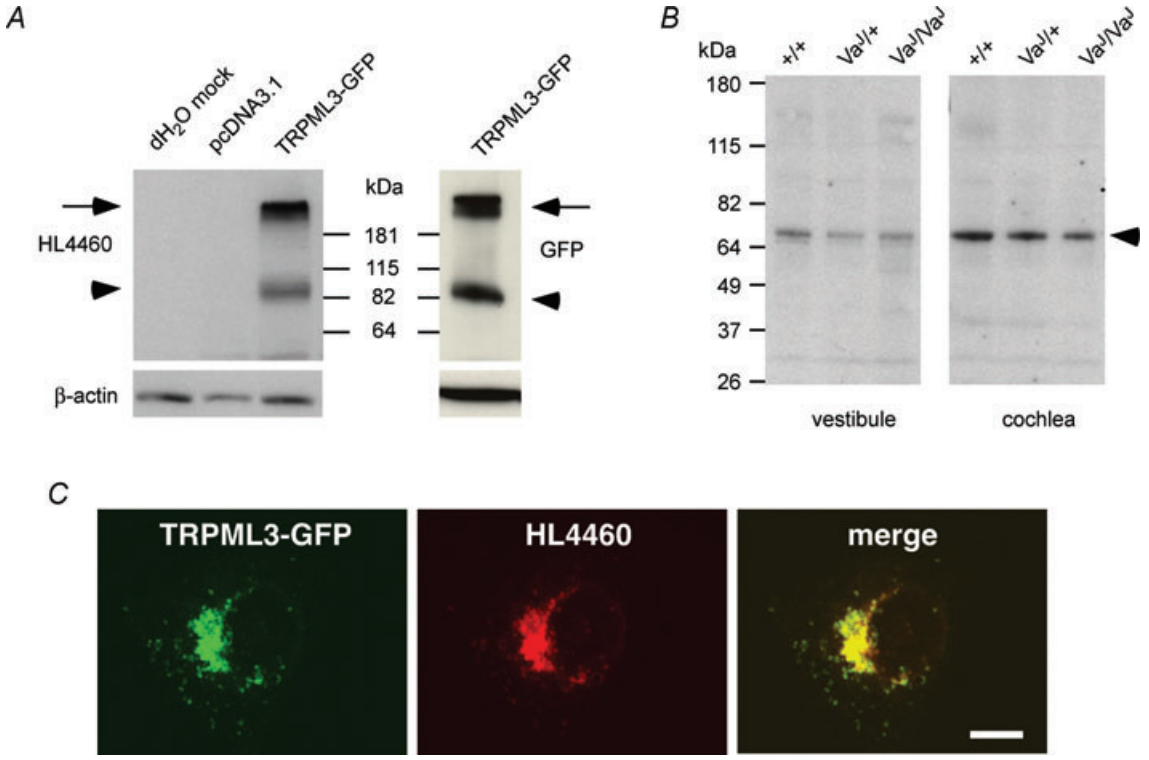

Figure 1. TRPML3 expression *in vitro* and in the inner ear
A, COS-1 cells were transfected with TRPML3-GFP and probed by Western blotting for the presence of fusion protein with HL4460 or anti-GFP. HL4460 detects GFP-tagged TRPML3 (arrowhead) of ∼91 kDa and a putative dimer at ∼215 kDa (arrow). The GFP antibody detects both the 91 kDa (arrowhead) and 215 kDa (arrow) bands. dH_2O mock and pcDNA3.1 represent transfection controls. Protein extracts (25 μg) were loaded in each lane. Equal loading and transfer efficiencies were evaluated with β-actin antibody. *B*, cochlear and vestibular tissue extracts from wild-type (+/+), heterozygous (Va^J/+) and homozygous (Va^J/Va^J) varitint-waddler mice, taken at P21, were probed for the presence of endogenous TRPML3 with HL4460. On Western blots, the 68 kDa TRPML3 species was present in both tissues (arrowhead) for all genotypes. Quantities of 25 μg and 40 μg were loaded in each lane for cochlear and vestibular extracts, respectively. *C*, transfected COS-1 cells expressing TRPML3-GFP (green) were stained with the HL4460 antibody (red). GFP fluorescence co-localizes with HL4460 labelling (merge). Scale bar in C = 10 μm

preparations of postnatal mice with the HL4460 and PB221 antibodies. In wild-type C3HeB/FeJ mice aged between postnatal days 2 and 6 (P2–P6), HL4460 stained a discrete region of the stereociliary bundle of IHCs and OHCs (Fig. 2*A*). Labelling was observed with both antibodies in the basal and apical coils of the organ of Corti. To obtain more precise information about the localization higher-resolution images were obtained (Fig. 2*B*–*D*). A higher magnification, viewed from the modiolar side, of IHCs and OHCs located in the apical coil revealed a uniform band of discrete label near the base of the stereocilia (Fig. 2*B* and *C*). Imaging OHCs from the top identified the staining as a double row of label that evenly outlined the stereociliary bundle (Fig. 2*D*). Similar results were obtained at ages P4–P6 (data not shown). By age P10, staining with HL4460 was absent in IHCs (Fig. 2*E*) and OHCs along most of the cochlear duct, with the exception of immature hair bundles located at the extreme apex of the organ of Corti (data not shown).

The localization of TRPML3 at the base of the stereocilia was confirmed by immunogold labelling, using the PB221 antibody (Fig. 3*A* and *B*). Gold particles were mainly observed in the ankle-link region at the base of the stereocilia. Controls with non-immune rabbit IgG showed no labelling (Fig. 3*C*).

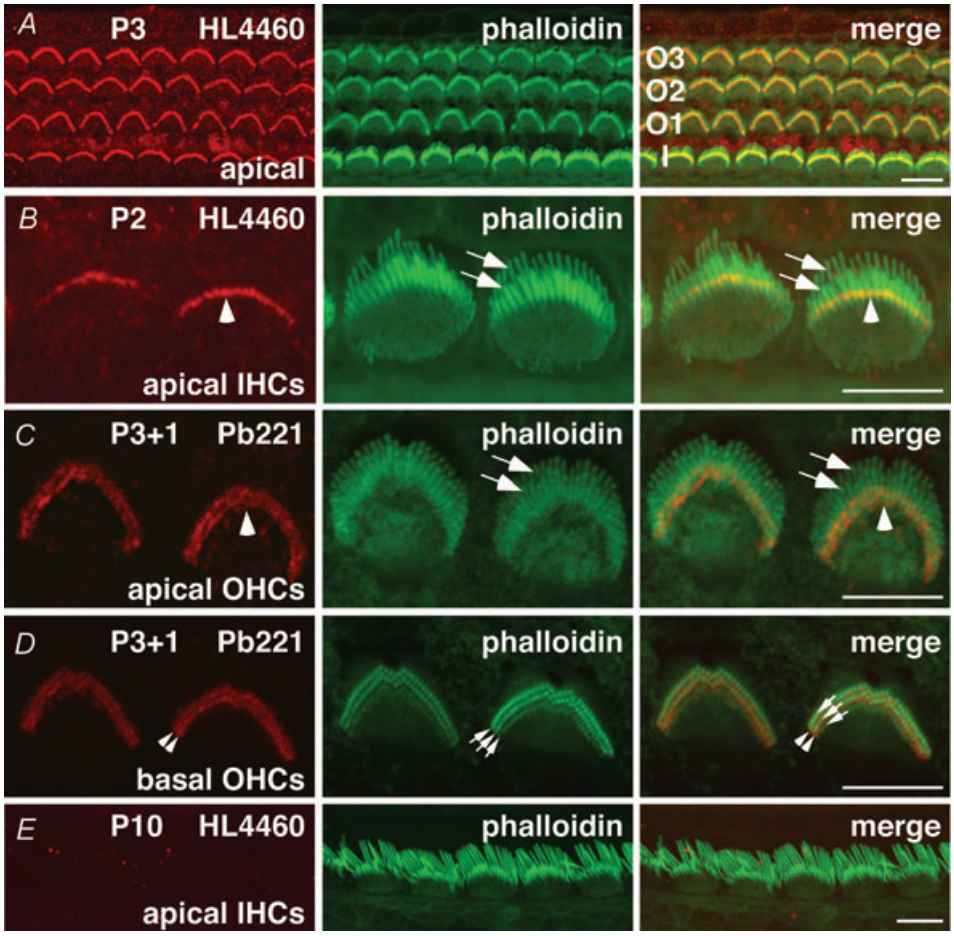

Figure 2. TRPML3 localization in cochlear hair cell stereocilia
Confocal images showing stereocilia of IHCs and OHCs of postnatal C3HeB/FeJ mice stained for TRPML3 (HL4460 or PB221; red) and F-actin (phalloidin; green). *A*, modiolar view of three rows of OHCs (labelled O1 to O3) and one row of IHCs (labelled I) of the apical region of the organ of Corti of a P3 mouse stained for TRPML3 and F-actin shows a discrete band of punctate staining of stereocilia on OHCs and IHCs. *B* and *C*, a higher magnification modiolar view of the organ of Corti (apical coil) stained for TRPML3 and F-actin shows discrete labelling at the base of stereocilia on IHCs (*B*, arrowhead) and OHCs (*C*, arrowhead). Arrows show tips of the stereocilia. *D*, top view of three rows of OHCs (basal coil) stained for TRPML3 and F-actin shows two rows of punctate staining (arrowheads) in each hair bundle in between three rows of stereocilia (arrows). *E*, modiolar view of one row of IHCs from the mid-apical region of P10 mice stained for TRPML3 and F-actin shows no discrete labelling of stereocilia. Scale bar in all images corresponds to 5 μm.

TRPML3 is absent from the stereocilia of *Va*^{J} mutants

In P3 +/+ mice the hair bundles of IHCs and OHCs present with a mature structure, showing staggered rows of stereocilia on IHCs and the V- or W-shape, which is the characteristic feature of the bundle on OHCs (Fig. 4*A*). In *Va*^{J}/+ mice, stereocilia on IHCs were severely splayed and distributed across the entire apical surface of the cell. On OHCs, the hair bundle had the recognizable mature form but showed signs of deterioration, which were most prominent on bundles of the outermost, third, row of OHCs. A disorientation of the bundle on OHCs was also frequently observed (Fig. 4*B*). In *Va*^{J}/*Va*^{J} IHCs and OHCs the hair bundles had entirely lost their mature appearance and were fully splayed and spread out over the apical surface (Fig. 4*C*). Stereocilia on OHCs formed irregular clusters across the surface (Fig. 4*C*).

To determine the effects of the *Va*^{J} point mutations (I362T/A419P) on TRPML3 localization, whole mounts of organs of Corti of varitint-waddler mutants were immunostained. At P3 in +/+ mice on OHCs and IHCs discrete staining of the stereocilia, as shown in more detail in Fig. 2, was observed (Fig. 4*A*). This staining, however, was not detectable in *Va*^{J}/+ or in *Va*^{J}/*Va*^{J} mutants (Fig. 4*B* and *C*). Similar results were obtained on specimens from P5 mice (data not shown). Multiple organs of Corti from *Va*^{J}/+ ($n > 5$) and *Va*^{J}/*Va*^{J} ($n > 5$) of P3 and P5 mice were analysed, but no specific staining of stereocilia was observed.

Varitint-waddler hair cells have impaired mechano-electrical transduction

The localization of TRPML3 in the hair bundles and the stereociliary defects in varitint-waddler mice suggested a potential adverse effect on hair-bundle mechanosensitivity. To investigate this hypothesis, we attempted to elicit transducer currents from apical OHCs (P3–P6) of mutant (*Va*^{J}/*Va*^{J} and *Va*^{J}/+) and wild-type (+/+) mice with sinusoidal mechanical stimulation (Kros *et al.* 1992). Control OHCs responded with large inward transducer currents at negative membrane potentials, up to −450 pA at −104 mV, when the hair bundles were deflected towards the kinocilium (the excitatory direction) (Fig. 5*A* and *E*). When the bundles were moved in the inhibitory direction, any transducer channels open in the absence of mechanical stimulation closed, resulting in a reduction of the inward current. Starting from −104 mV and stepping the membrane potential to more depolarized values, the transducer currents initially decreased in size and then reversed at +6.6 ± 0.8 mV ($n = 3$). For more positive membrane potentials, fluid jet stimuli in the excitatory direction caused outward currents and the transducer current activated at rest increased, a sign of reduced adaptation of the transducer current upon approaching the Ca^{2+} equilibrium potential (Assad *et al.* 1989; Crawford *et al.* 1989). Note the opposite direction of the hysteresis at negative and positive holding potentials in the plots of Fig. 5*E*, which has been noted before for

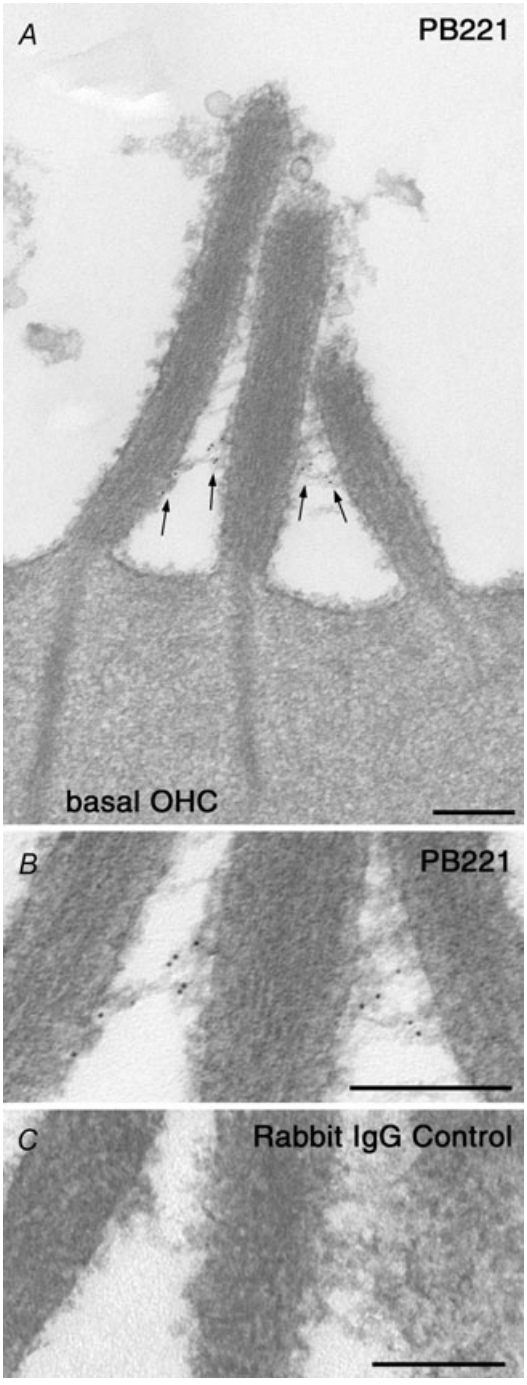

Figure 3. TRMPL3 labelling in the ankle-link region of stereocilia
A, electron micrograph of an OHC hair bundle from a cochlear culture labelled with rabbit antibody PB221 to the ectodomain of TRPML3 followed by 10 nm gold-conjugated goat anti-rabbit. The gold particles are observed in the ankle-link region (arrows) at the base of the hair bundle. *B*, detail of ankle-link region shown above in *A*. Scale bars = 200 nm. *C*, labelling is not seen in the control with non-immune rabbit IgG.

transducer currents elicited by sine wave stimuli (Kros *et al.* 1993). The clockwise hysteresis at negative potentials is due to a degree of adaptation whereas the counter-clockwise hysteresis at positive potentials can be attributed to slow current offsets that have been described following step stimuli (Crawford *et al.* 1989).

In keeping with their moderately disorganized hair bundles (Fig. 4*B*), OHCs from heterozygous mice had mechanosensitive currents that were smaller than control currents but with current–voltage relationships that were similar in shape (Fig. 6*A*), including an increase in resting transducer current upon depolarization (Fig. 5*B* and *F*). At −104 mV, transducer currents ranged from −70 to −190 pA in $Va^J/+$ mice ($n = 9$). This cell showed no evidence of adaptation during the sinusoidal stimuli at −104 mV as the hysteresis was clockwise at both potentials, possibly as a consequence of the small transducer currents (Ricci & Fettiplace, 1997). Although the bundles of the homozygous mutant OHCs appeared extremely irregular, lacking the normal V- or W-shape (Fig. 4*C*), they were, at least in the apical coil, usually clearly recognizable. Only cells with recognizable bundles were selected for electrophysiological recordings. Transducer currents were, however, absent in 20 out of 22 homozygous Va^J/Va^J OHCs (Fig. 5*C*) from animals aged P3 or older. In two Va^J/Va^J OHCs small, saturating transducer currents of −75 and −145 pA at −104 mV were recorded, with no resting transducer current (Fig. 5*D* and *G*). At extreme positive potentials, a resting transducer current became evident in both cells. Again, there was no sign of adaptation during the sinusoidal stimuli. Figure 6*A* shows average current–voltage curves for the peak-to-peak transducer currents of all cells.

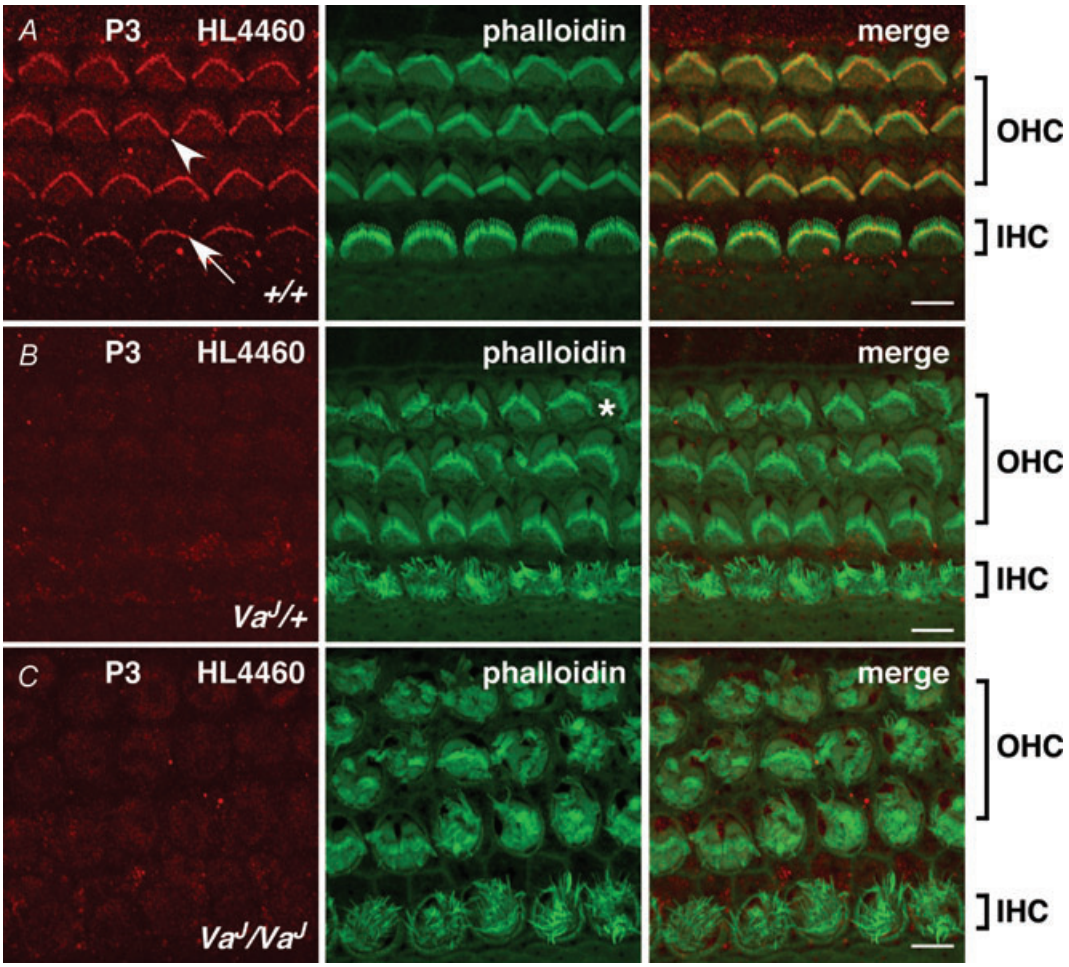

Figure 4. TRPML3 localization in varitint-waddler auditory hair cells
Confocal images showing stereocilia of IHCs and OHCs of P3 mice of +/+ (*A*), $Va^J/+$ heterozygotes (*B*), and Va^J/Va^J homozygotes (*C*) stained for TRPML3 (HL4460, red) and F-actin (phalloidin, green). Discrete labelling is observed in wild-type +/+ mice at stereocilia of OHCs (arrowhead) and IHCs (arrow), but not in the stereociliary hair bundle of $Va^J/+$ and Va^J/Va^J mutants. All images taken from middle of apical coil. The star indicates a disoriented hair bundle. Scale bar in all images corresponds to 5 μm.

Homozygous varitint-waddler hair cells are depolarized by an inwardly rectifying leak current

The transduction experiments, which were usually carried out using a Cs^+-based intracellular solution in order to minimize basolateral K^+ currents and thus to enable large depolarizations without significant voltage drops across the series resistance, also showed evidence of another effect of the mutation, namely the inwardly rectifying leak conductance which we first reported for homozygous (Va^J/Va^J) OHCs in Grimm *et al.* (2007) (see Fig. 5*C* and *D*). Given that the heterozygous $Va^J/+$ OHCs had reduced transducer currents, it was important to investigate whether they also expressed the leak conductance. The leak was not detectable in wild-type (+/+) or heterozygous ($Va^J/+$) hair cells (Fig. 5*A* and *B*, and 6*B*). The inward current at −104 mV was some 10 times larger in homozygotes than either wild-type ($P < 0.01$) or heterozygotes ($P < 0.001$), whereas at +96 mV the outward current in homozygotes was slightly smaller than wild-type ($P < 0.05$) or heterozygotes (difference not significant).

To investigate the extent to which the inwardly rectifying leak conductance depolarized the OHC resting potentials, a series of experiments was conducted using a more physiological, K^+-based intracellular solution (Fig. 7*A*–*C*). Both wild-type (+/+) and heterozygous ($Va^J/+$) OHCs (Fig. 7*A* and *B*) had small holding currents at −84 mV and depolarizing voltage steps elicited time- and voltage-dependent K^+ currents ($I_{K,neo}$) as described before (Marcotti & Kros, 1999). The homozygous mutant (Va^J/Va^J) OHCs again had large inward holding currents at −84 mV and depolarizing voltage steps showed instantaneous currents of progressively smaller size, followed for potentials positive to about −40 mV by a smaller than normal $I_{K,neo}$ (Fig. 7*C*).

Figure 8*A* shows average steady-state current–voltage curves of experiments with K^+-based intracellular solutions like those shown in Fig. 7. It is clear that the homozygous mutant (Va^J/Va^J) OHCs have larger inward currents at hyperpolarized potentials and smaller outward K^+ currents than their wild-type and heterozygote counterparts. Inward current at −104 mV was about six times larger in the homozygotes than wild-type ($P < 0.01$) and heterozygotes ($P < 0.001$). The outward current at about +40 mV was, by contrast, three times smaller in the homozygotes relative to wild-type and heterozygotes ($P < 0.001$ in both cases). The reduced size of $I_{K,neo}$ in Va^J/Va^J mutant OHCs (Figs 7*C* and 8*A*) may conceivably be due to a slow inactivation at the depolarized resting potentials of these cells. Partial inactivation of this current has been observed (Marcotti & Kros, 1999; Helyer *et al.* 2005).

Resting potentials, measured as zero-current potentials (V_z), were -54 ± 4 mV (+/+, $n = 7$), -52 ± 2 mV ($Va^J/+$, $n = 18$), and -33 ± 2 mV (Va^J/Va^J, $n = 20$) (Fig. 8*B*). Zero-current potentials were significantly different between the Va^J/Va^J mutants on the one hand and $Va^J/+$ and wild-type on the other (both $P < 0.001$). For currently unknown reasons, the leak conductance of Va^J/Va^J OHCs appeared significantly larger ($P < 0.01$) when Cs^+ rather than K^+ was the main intracellular cation (Fig. 8*C* and *D*). The leak conductance, measured as the slope conductance at −84 mV and using a K^+-based intracellular solution, was 15.5 ± 3.3 nS for Va^J/Va^J OHCs ($n = 15$) (Fig. 8*C*). With Cs^+-based intracellular solution the leak conductance was 31.4 ± 4.6 nS ($n = 23$) (Fig. 8*D*). It is probable that open TRPML3 mutant channels in homozygous varitint-waddler mice are the underlying cause of the large leak currents (Grimm *et al.* 2007; Kim *et al.* 2007). The much smaller ($P < 0.001$) residual leak currents of around 3 nS in $Va^J/+$ and wild-type mice using either intracellular solution (Fig. 8*C* and *D*) are likely to flow through other channel types. The homozygous mutant OHCs appeared considerably more fragile than wild-type OHCs and it was difficult to maintain whole-cell recordings for longer than a few minutes, possibly due to Na^+ and Ca^{2+} loading through the leak conductance.

Separating leak and mechano-electrical transducer currents

Experiments with permeant transducer-channel blockers were carried out to investigate whether there were any similarities between the inwardly rectifying leak current and the mechano-electrical transducer current. FM1-43 dye rapidly enters mouse cochlear hair cells via transducer channels (Gale *et al.* 2001; Meyers *et al.* 2003), labelling therefore being an indication of transducer channels open at rest. Loading of FM1-43 in control (+/+) hair cells (Fig. 9) was normal and indistinguishable from that previously observed in wild-type CD1 control cultures (Gale *et al.* 2001). However, dye loading in the hair cells of homozygous (Va^J/Va^J) mutant hair cells was abolished (Fig. 9), consistent with either transducer current–voltage curves being shifted to the right or with the absence of mechanosensitivity. Heterozygous mutants showed reduced dye loading with some variability between cells (Fig. 9), consistent with the observation that their transducer currents were reduced to a variable extent. Similarly, aminoglycosides are permeant blockers of the transducer channel (Marcotti *et al.* 2005). The uptake of radionucleotide-labelled gentamicin was examined using grain-density autoradiography. In sections from the basal and mid-apical coils, intense labelling was observed over the OHCs and, to a slightly lesser degree, over the IHCs (Fig. 10). This labelling was not detectable (i.e. reduced to background levels) in homozygous (Va^J/Va^J) mutant hair cells (Fig. 10), again supporting the conclusion that mechanosensitivity is either absent or that current–voltage

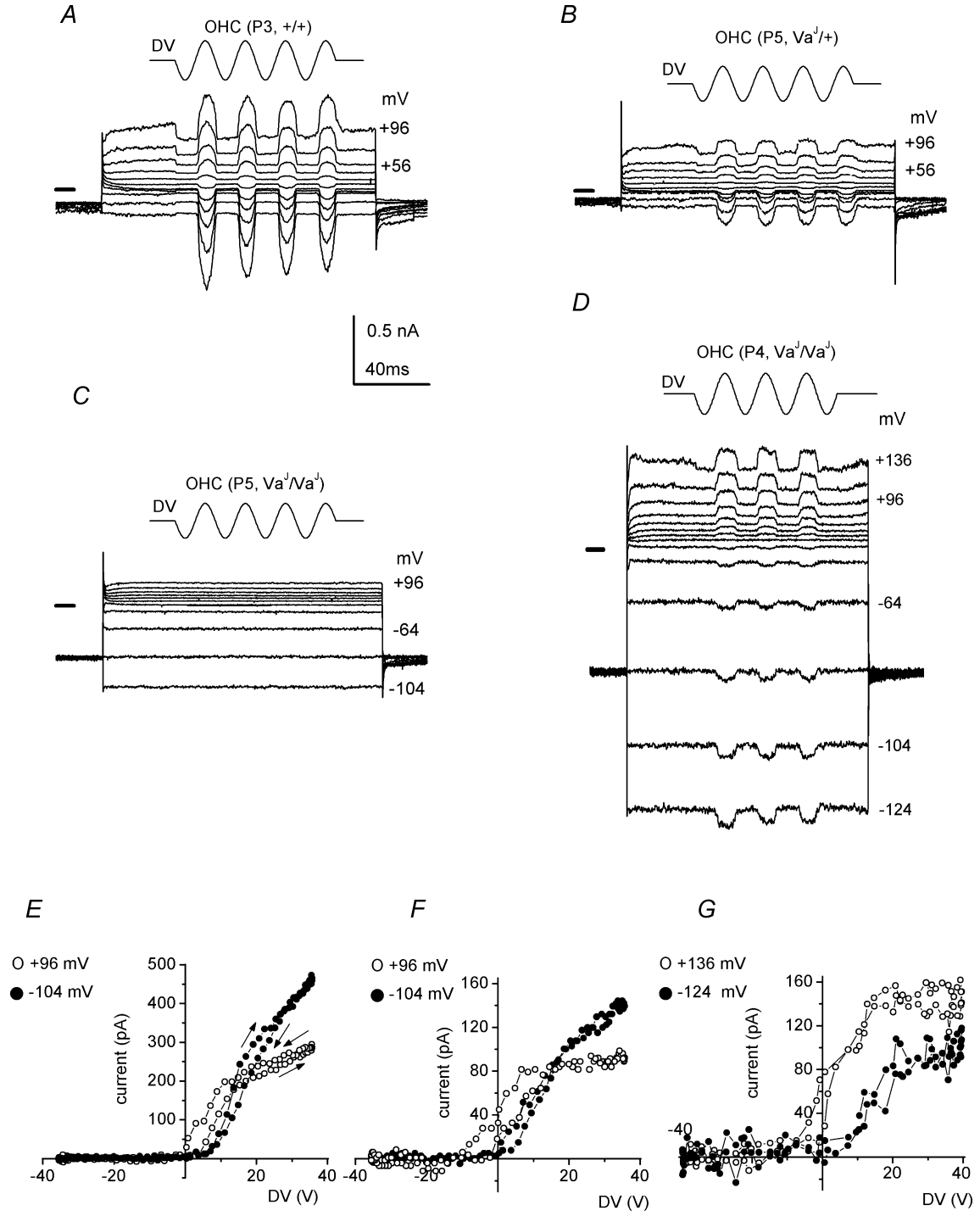

Figure 5. Transducer currents at different membrane potentials recorded from +/+, *Va*^{J}/+ and *Va*^{J}/*Va*^{J} OHCs

Transducer currents were recorded in response to 45 Hz sinusoidal force stimuli. Cells were held at −84 mV and the membrane potential was stepped to different levels in 20 mV increments. Driver voltage to the fluid jet is shown above the traces, upward being excitatory. Membrane potentials are shown next to some of the traces. *A*, P3 +/+ OHC; *B*, P5 *Va*^{J}/+ OHC; *C*, P5 *Va*^{J}/*Va*^{J} non-transducing OHC; *D*, P4 *Va*^{J}/*Va*^{J} transducing OHC. Driver voltage amplitude 40 V in *D*. Note the large 'leak' conductance in *C* and *D*. All recordings are from apical coil OHCs. Horizontal bars left of the recordings indicate zero-current level. Some spike artefacts in the currents of *B* and *C* have been blanked. *E*–*G*, absolute value of transducer currents as a function of driver voltage for the cells

curves are shifted to the right. In cultures prepared from heterozygous ($Va^J/+$) mice the labelling was reduced but still present (Fig. 10). Clearly, neither FM1-43 nor gentamicin entered hair cells through the leak conductance in Va^J/Va^J hair cells under our experimental conditions.

To try and characterize the leak current further, we tested the effects of FM1-43 and aminoglycoside antibiotics on the electrophysiological recordings of OHCs in acutely isolated organs of Corti. The leak conductance in the Va^J/Va^J OHCs remained in the presence of 100 μM neomycin (18.8 ± 12.1 nS at -84 mV, $n = 2$) or 10 μM FM1-43 (41.7 ± 6.9 nS, $n = 4$). The matching zero-current potentials (all using K^+-based intracellular solution) were depolarized, -34 ± 0 mV and -35 ± 3 mV, respectively. Aminoglycosides and FM1-43 are open-channel blockers of the hair-cell transducer channel (Gale *et al.* 2001; Marcotti *et al.* 2005), thereby again differentiating the leak conductance from the mechanosensitive conductance. Also, at P0 transducer currents are not yet present in apical coil OHCs in the mouse (W. Marcotti, G. P. Richardson & C. J. Kros, unpublished observations), but in one P0 Va^J/Va^J OHC a large inward leak current was already observed, with a conductance of 12.1 nS around -84 mV.

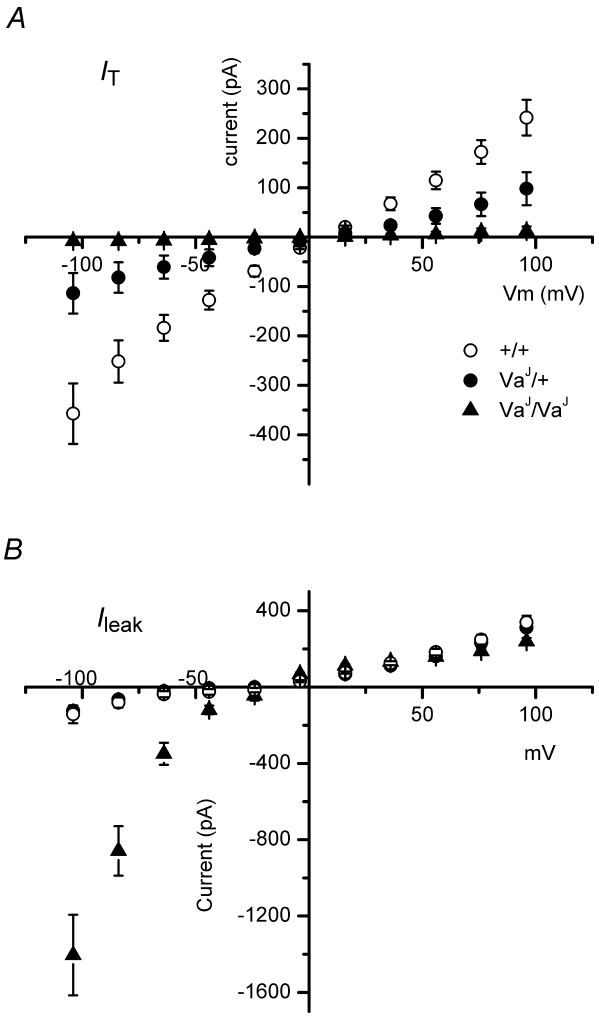

Figure 6. *I–V* relationships for transducer and leak currents from +/+, $Va^J/+$ and Va^J/Va^J OHCs
A, averaged mechano-electrical transducer currents for +/+ ($n = 3$, P3), $Va^J/+$ ($n = 9$, P5) and Va^J/Va^J ($n = 22$, P3–6) OHCs. *B*, averaged leak currents for +/+ ($n = 7$, P3–5), $Va^J/+$ ($n = 9$, P5) and Va^J/Va^J ($n = 23$, P0–6) OHCs. Holding potential was -84 mV. From *A* it is clear that Va^J/Va^J OHCs display negligible transducer currents. Transducer currents in the heterozygous cells are of a lower amplitude when compared to the wild-type control cells. *B* shows that +/+ and $Va^J/+$ cells have identical *I–V* relationships and do not display the inwardly rectifying leak current. The Va^J/Va^J cells display a strong rectifying leak current. Cs^+-based intracellular solution. Recordings are from apical ($n = 36$) and basal ($n = 3$) OHCs.

Discussion

In this study, we identified the location of TRPML3 in developing wild-type hair-cell stereocilia, demonstrated compromised mechanotransduction in varitint-waddler cochlear hair cells, and further investigated a constitutively active inward current that we identified before in these hair cells (Grimm *et al.* 2007). We propose that the progressive hair-cell degeneration in varitint-waddler mice is caused by constitutively open mutant TRPML3 isoforms.

Localization of TRPML3 near the ankle-link region of stereocilia

At P3 the stereociliary bundle of outer hair cells consists of three staggered rows of stereocilia arranged in a V-shape. The cohesiveness of the bundle is achieved by a network of fine extracellular filaments connecting neighbouring stereocilia at the base and along the shaft. The punctuated and double-row appearance of the HL4460 and PB221 staining suggests that TRPML3 localizes to the sides of stereocilia that face each other. This places TRPML3 near the region of the ankle-link filaments. Several other proteins have been shown by immunofluorescence to localize to this region, including radixin, usherin and vezatin (Küssel-Andermann *et al.* 2000; Pataky *et al.* 2004; Adato *et al.* 2005; Michalski *et al.* 2007). However, the location of TRPML3 shows conspicuous similarity

of *A*, *B* and *D*, respectively, averaged during two stimulus periods, starting with the negative half-cycle. The resting transducer currents (before stimulus onset) are 11 pA at -104 mV and 87 pA at +96 mV (*E*); 6 pA at -104 mV and 50 pA at +96 mV (*F*); 7 pA at -124 mV and 61 pA at +136 mV (*G*). Filled symbols: currents at most negative potential used; open symbols: currents at most positive potential. Data points are at 200 μs intervals. Arrows in *E* indicate stimulus direction.

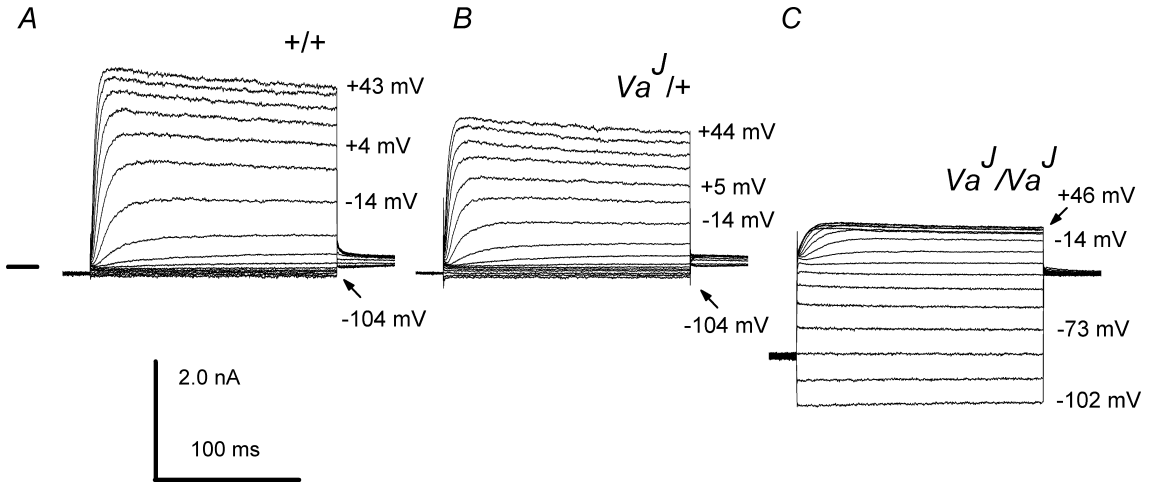

Figure 7. Basolateral currents at different membrane potentials recorded from +/+, *Va*^{J}/+ and *Va*^{J}/*Va*^{J} OHCs

Basolateral currents were elicited by voltage steps in 10 mV increments from a holding potential of −84 mV, nominally between −104 mV and +46 mV. Following the steps the potential was returned to −44 mV. Membrane potentials (corrected for series resistance) are shown next to some of the traces. *A*, P3 +/+ OHC; *B*, P3 *Va*^{J}/+ OHC; *C*, P4 *Va*^{J}/*Va*^{J} OHC. Note the large inwardly rectifying leak conductance in *C*. Recordings are from apical and basal coil OHCs. Horizontal bar left of the recording in *A* indicates zero-current level for all panels.

with the position of VLGR1, which is a G-protein receptor-coupled transmembrane protein with a very large extracellular domain that was recently shown to form the ankle-link filaments (McGee *et al.* 2006). Furthermore, the stereociliary defects caused by mutations in *Vlgr1* are similar to those seen in varitint-waddler hair cells (Johnson *et al.* 2005; McGee *et al.* 2006) and both TRPML3 and VLGR1 disappear from the ankle region around P8 (Michalski *et al.* 2007). This transient expression of TRPML3 and VLGR1 correlates with that of the ankle links themselves (McGee *et al.* 2006). This suggests that TRPML3 may contribute to the regulation of the micro-environment of the developing hair bundle, strategically positioned at the ankle-link region. How exactly this

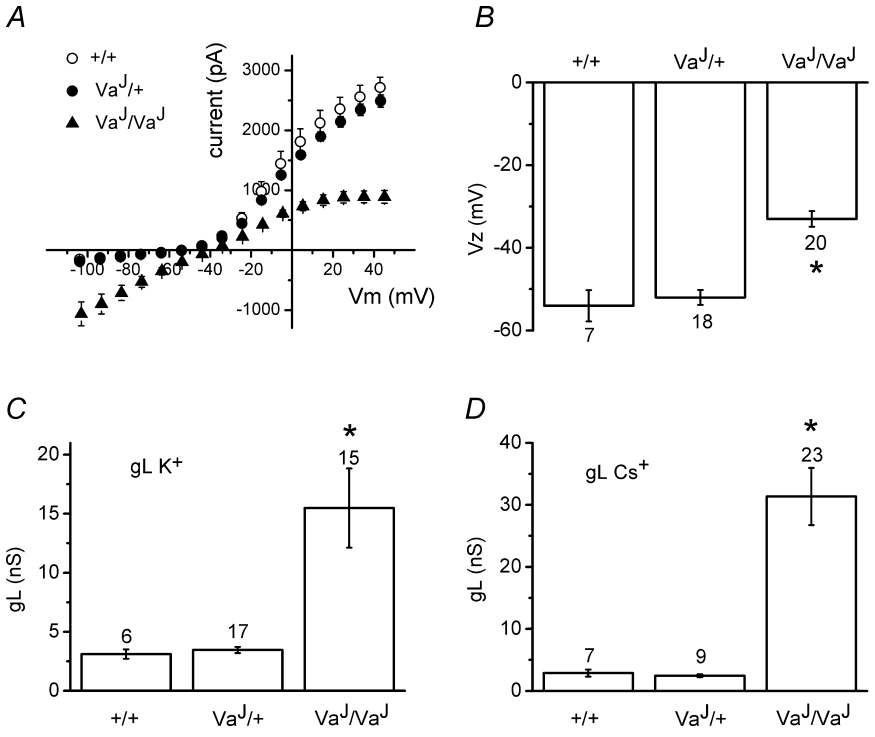

Figure 8. Effects of the inwardly rectifying leak conductance on *Va*^{J}/*Va*^{J} OHCs

A, *I–V* relationships using K^+-based intracellular solution. Averaged currents ± S.E.M. of +/+ ($n = 5$, P3–5), *Va*^{J}/+ ($n = 10$, P2–5) and *Va*^{J}/*Va*^{J} ($n = 11$, P1–6) OHCs. From a holding potential of −84 mV the voltage was stepped in 10 mV increments from −104 mV to +46 mV nominally (error bars for voltage are hidden by the symbols). *B*, average zero-current potentials with K^+-based intracellular solution of +/+ ($n = 7$, P3–5), *Va*^{J}/+ ($n = 18$, P2–5) and *Va*^{J}/*Va*^{J} ($n = 20$, P1–6) OHCs (*$P < 0.001$). *C*, average leak conductance with K^+-based intracellular solution of +/+ ($n = 6$, P3–5), *Va*^{J}/+ ($n = 17$, P2–5) and *Va*^{J}/*Va*^{J} ($n = 15$, P1–6) OHCs (*$P < 0.001$). *D*, average leak conductance using Cs^+-based intracellular solution of +/+ ($n = 7$, P3–5), *Va*^{J}/+ ($n = 9$, P5) and *Va*^{J}/*Va*^{J} ($n = 23$, P0–6) OHCs (*$P < 0.001$).

regulation would occur is currently not clear, but the unusual regulation of the activity of the native channel by changes in extracellular Na^+ concentration (Kim *et al.* 2007) points to a possible role in signalling changes in endolymph composition which occur during the first postnatal week (Anniko & Wroblewski, 1986).

The structure of the hair bundle in varitint-waddler homozygotes is profoundly disrupted. Staining of mutant stereocilia was consistently at background level without revealing a discrete localization. It has been shown *in vitro* that the TRPML3<I362T/A419P> isoform shows low levels of surface expression (Grimm *et al.* 2007; Kim *et al.* 2007). This suggests that in Va^J homozygotes, TRPML3 may not be targeted to stereocilia, which is in agreement with our immunolocalization data. In Va^J heterozygotes, however, we expected to detect the wild-type isoform, even more so since some hair bundles in heterozygotes had a fairly normal appearance and they did transduce. It is known that TRP channels form multimers consisting of four subunits to function (Clapham, 2003) and therefore it is possible that complexes containing only wild-type isoforms are targeted to the stereocilia. Assuming a random incorporation of subunits, only 6.25% of channel tetramers contain exclusively wild-type subunits and would thus be targeted correctly. The reduced number of correctly localized subunits could be below the detection limit of the antibodies.

Defective mechano-electrical transduction and the nature of the leak conductance in Va^J mutants

The absent or greatly reduced transducer currents in the homozygous mutant OHCs are likely to be primarily a consequence of the severely compromised ultrastructure of the hair bundles. We applied high concentrations of transducer channel blockers in an effort to distinguish between the transducer channel and TRMPL3. Whereas the absence of FM1–43 uptake in response to a brief, 10 s application in cultures might be due to failure of the drug to reach mislocated channels in the basolateral membrane, the absence of gentamicin uptake when applied for 2 h in the Va^J/Va^J mutant hair cells and the persistence of the leak conductance when FM1-43 or neomycin were bath-applied for between 5 and 30 min in acutely isolated organs of Corti, suggest that mutated TRPML3 is a separate entity from the mechano-electrical transducer channel. An alternative interpretation is that the leak conductance in the Va^J/Va^J OHCs might represent an aberrant form of the transducer channel, which has lost mechanosensitivity and acquired altered permeation properties (inward rectification and reduced sensitivity to transducer channel blockers). A precedent for changes of this kind is set by mutations in ENaC channels (Fuller *et al.* 1997). The normal localization of TRPML3 near the ankle links might in that case represent a 'reserve pool' of transducer channels. This possibility is rendered unlikely by the recently reported single-channel conductance of both native TRPML3 and TRPML3<A419P> of about 50 pS at physiological potentials in 2 mM extracellular Ca^{2+} (Xu *et al.* 2007; Nagata *et al.* 2008), considerably smaller than the values of over 100 pS reported for the OHC transducer channel (Geleoc *et al.* 1997; Beurg *et al.* 2006). An additional possibility is that the transducer currents may be shut off by strong adaptation in Va^J/Va^J OHCs. This assumes that the stereocilia may be Ca^{2+}-loaded due to their depolarized resting potentials as a consequence

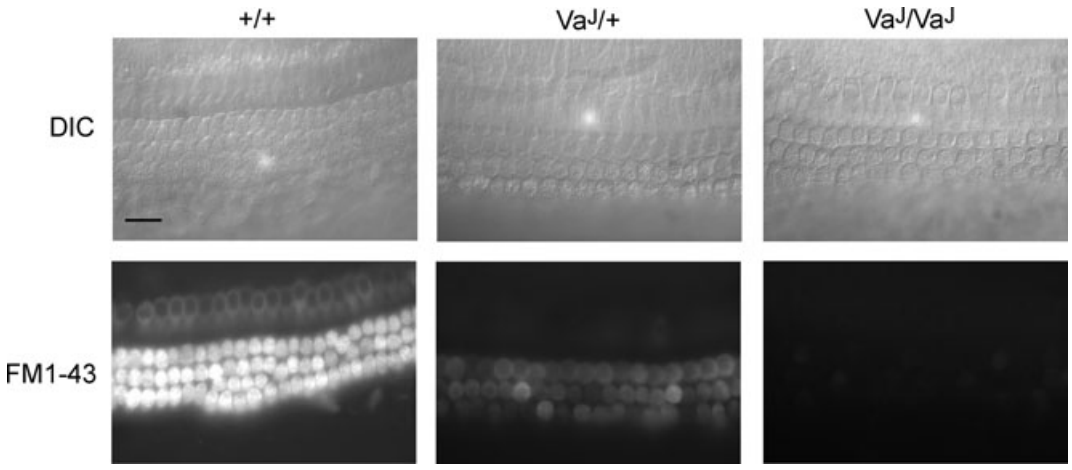

Figure 9. Failure of homozygous varitint-waddler hair cells to load with FM1-43
Top panels show DIC images from basal coil cochlear cultures (P1, 1 day *in vitro*) from control (+/+) and mutant ($Va^J/+$ and Va^J/Va^J) mice. Bottom panels are images taken between 10 and 20 min after a 10 s bath application of 3 μM FM1-43 from the same cultures shown in the top panels. Control hair cells load avidly with FM1-43 whereas heterozygous and homozygous mutant hair cells show reduced dye labelling and fail to load, respectively. Scale bar = 20 μm.

of the leak conductance. This cannot, however, explain the reduction of the transducer currents in the $Va^J/+$ mutants (Fig. 5*B*), as they do not express the leak conductance and have normal resting potentials. From the immunolabelling and electrophysiological findings (corroborated by the FM1-43 and gentamicin uptake experiments) in the heterozygotes, it would thus appear that the absence of TRPML3 in the hair bundle by itself reduces mechano-electrical transducer currents, even in the absence of the leak conductance. Apart from their small size the transducer currents appear normal, suggesting a reduction in the number of otherwise normal transducer channels due to the hair-bundle defects.

The inward rectification of the leak conductance in OHCs of homozygous varitint-waddler mice is similar to that of the constitutively open channels found when mutant TRPML3 protein is expressed in HEK 293 (Grimm *et al.* 2007; Kim *et al.* 2007; Xu *et al.* 2007) or LLC-PK1-CL4 cells (Nagata *et al.* 2008), indicating that the leak channels in the OHCs are likely to consist of mutated TRPML3 subunits. The largest values of the leak conductance that we observed (46 nS in K^+- and 75 nS in Cs^+-based intracellular solution) suggest that the number of leak channels that can be present in the cell membrane is in the order of a thousand. We postulate that this leak conductance is responsible for the eventual cell death in the Va^J/Va^J mutants through depolarization which leads to Ca^{2+} loading and thereby the demise of the cells during the first postnatal weeks (Cable & Steel, 1998).

An alternative explanation for the leak conductance, in both OHCs and the expression systems, is that it might not pass through the mutated TRPML3 channels themselves, but that accumulation of mutant TRMPL3 in the cells due to impaired targeting to the cell membrane (Grimm *et al.* 2007; Kim *et al.* 2007) might trigger the endoplasmic reticulum stress response (Szegezdi *et al.* 2006), which

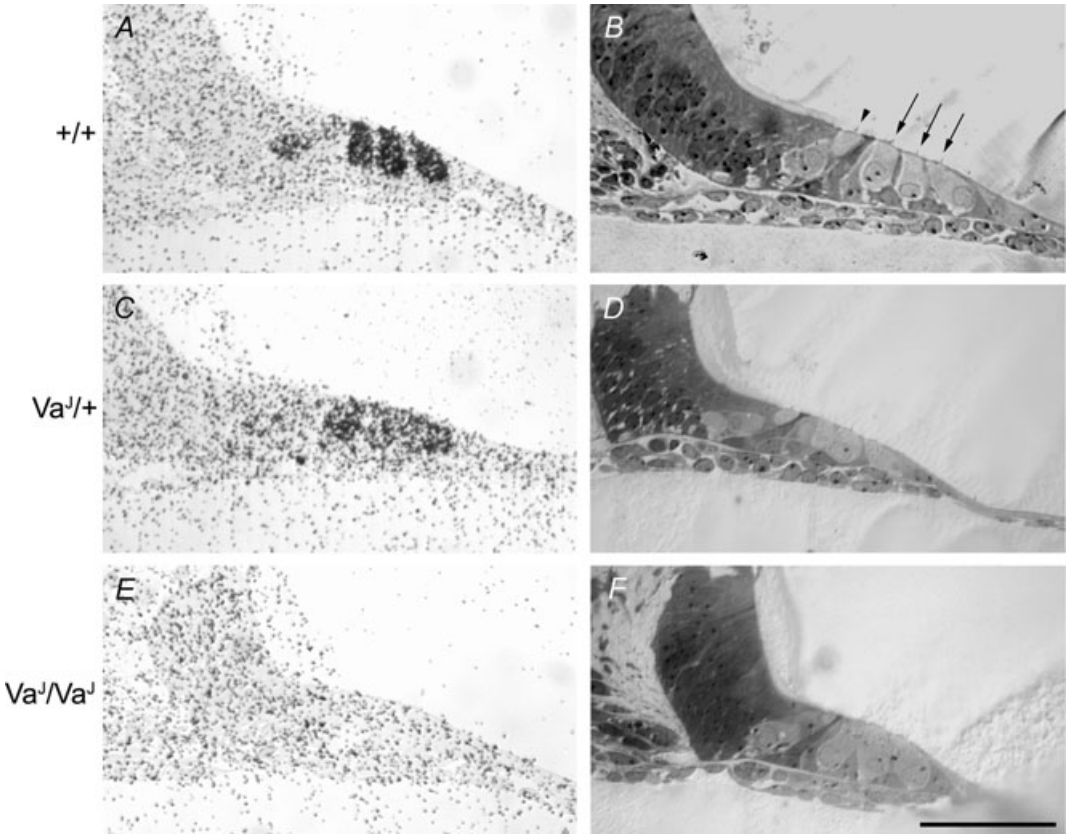

Figure 10. Impaired tritiated gentamicin uptake in Va^J mutants
A progressive decrease in tritiated gentamicin uptake is observed from wild-type to homozygous hair cells. Hair cells in the basal coil of P3 wild-type cochleae take up aminoglycosides. Cells that are labelled (*A*) correspond with the inner and outer hair cells shown using toluidine staining in *B*. Heterozygote P3 cochlear basal coil hair cells exhibit less labelling following incubation with gentamicin (*C*) than those in wild-types. Sections of heterozygote cochleae were also stained with toluidine to show the localization of IHCs and OHCs (*D*). IHCs in both wild-type (*A*) and heterozygote (*C*) sections take up less gentamicin than OHCs. Basal coil hair cells in homozygote cochleae do not take up aminoglycosides (*E*). Mutant hair cells can be seen using toluidine staining (*F*). Arrowhead, IHC; arrows, OHCs. Scale bar = 100 μm.

could conceivably in turn somehow lead to activation of endogenous channels unrelated to TRPML3. We consider this less likely for three reasons: (1) the close similarity of the inwardly rectifying currents in two different expression systems and OHCs, with near-perfect overlap of the *I–V* relationships in HEK 293 cells and OHCs (Grimm *et al.* 2007); (2) the similar inward rectification found in native and mutant TRPML3 (Kim *et al.* 2007, 2008); and (3) the identical single-channel conductance of native and mutant TRPML3 (Nagata *et al.* 2008).

The absence of antibody labelling in the *Va*^{J}/*Va*^{J} mutants suggests that the leak channels are misdirected away from the ankle-link region of the hair bundles, but given the presence of the leak conductance some of them must still be expressed in the cell membrane, perhaps diffusely over the basolateral membrane. The lack of a measurable leak conductance in the *Va*^{J}/+ mutants, where TRPML3 is also misdirected away from the bundles, suggests that all four subunits must be mutated for a channel to become leaky, thus affecting only 6.25% of channels. We conclude that the varitint-waddler A419P substitution in transmembrane domain 5 of TRPML3 is associated with compromised mechanosensitivity in mammalian cochlear hair cells, which, in conjunction with the channel's normal stereociliary localization, is compatible with a role for TRPML3 in the organization of proper hair-bundle development as a requirement for normal mechanotransduction. The deafness in the *Va*^{J}/*Va*^{J} mutants, which lack compound action potentials and cochlear microphonics and have small or absent endocochlear potentials due to stria vascularis defects, is probably due to multiple factors. By contrast, the *Va*^{J}/+ mutants do not express the leak conductance and have much less severe hair-cell degeneration. They have no compound action potentials, small or absent cochlear microphonics but mostly normal endocochlear potentials (Cable & Steel, 1998). We suggest that their hearing loss is a likely consequence of hair-bundle defects due to the *Trpml3* mutations that lead to a reduction in the number of functional mechano-electrical transducer channels. Overall the evidence presented strongly suggests that TRPML3 can be removed from the short list of candidates for the mammalian hair-cell transducer channel (Corey, 2006).

References

Adato A, Lefevre G, Delprat B, Michel V, Michalski N, Chardenoux S, Weil D, El-Amraoui A & Petit C (2005). Usherin, the defective protein in Usher syndrome type IIA, is likely to be a component of interstereocilia ankle links in the inner ear sensory cells. *Hum Mol Genet* **14**, 3921–3932.

Anniko M & Wroblewski R (1986). Ionic environment of cochlear hair cells. *Hear Res* **22**, 279–293.

Assad JA, Hacohen N & Corey DP (1989). Voltage dependence of adaptation and active bundle movement in bullfrog saccular hair cells. *Proc Natl Acad Sci U S A* **86**, 2918–2922.

Atiba-Davies M & Noben-Trauth K (2007). TRPML3 and hearing loss in the varitint-waddler mouse. *Biochim Biophys Acta* **1772**, 1028–1031.

Beurg M, Evans MG, Hackney CM & Fettiplace R (2006). A large-conductance calcium-selective mechanotransducer channel in mammalian cochlear hair cells. *J Neurosci* **26**, 10992–11000.

Bryant JE, Marcotti W, Kros CJ & Richardson GP (2003). FM1-43 enters hair cells from the onset of mechano-electrical transduction in both mouse and chick cochlea. *Assoc Res Otolaryngol Abs*, 107.

Cable J & Steel KP (1998). Combined cochleo-saccular and neuroepithelial abnormalities in the Varitint-waddler-J (*Va*^{J}) mouse. *Hear Res* **123**, 125–136.

Clapham DE (2003). TRP channels as cellular sensors. *Nature* **426**, 517–524.

Cloudman AM & Bunker LE (1945). The varitint-waddler mouse. *J Hered* **36**, 258–263.

Corey DP (2006). What is the hair cell transduction channel? *J Physiol* **576**, 23–28.

Crawford AC, Evans MG & Fettiplace R (1989). Activation and adaptation of transducer currents in turtle hair cells. *J Physiol* **419**, 405–434.

Cuajungco MP, Grimm C & Heller S (2007). TRP channels as candidates for hearing and balance abnormalities in vertebrates. *Biochim Biophys Acta* **1772**, 1022–1027.

Denk W, Holt JR, Shepherd GM & Corey DP (1995). Calcium imaging of single stereocilia in hair cells: localization of transduction channels at both ends of tip links. *Neuron* **15**, 1311–1321.

Deol MS (1954). The anomalies of the labyrinth of the mutants varitint-waddler, shaker-2 and jerker in the mouse. *J Genet* **52**, 562–588.

Di Palma F, Belyantseva IA, Kim HJ, Vogt TF, Kachar B & Noben-Trauth K (2002). Mutations in *Mcoln3* associated with deafness and pigmentation defects in varitint-waddler (*Va*) mice. *Proc Natl Acad Sci U S A* **99**, 14994–14999.

Fuller CM, Berdiev BK, Shlyonsky VG, Ismailov II & Benos DJ (1997). Point mutations in alpha bENaC regulate channel gating, ion selectivity, and sensitivity to amiloride. *Biophys J* **72**, 1622–1632.

Gale JE, Marcotti W, Kennedy HJ, Kros CJ & Richardson GP (2001). FM1-43 dye behaves as a permeant blocker of the hair-cell mechanotransducer channel. *J Neurosci* **21**, 7013–7025.

Geleoc GS, Lennan GW, Richardson GP & Kros CJ (1997). A quantitative comparison of mechanoelectrical transduction in vestibular and auditory hair cells of neonatal mice. *Proc R Soc Lond B Biol Sci* **264**, 611–621.

Goodyear RJ, Marcotti W, Kros CJ & Richardson GP (2005). Development and properties of stereociliary link types in hair cells of the mouse cochlea. *J Comp Neurol* **485**, 75–85.

Grimm C, Cuajungco MP, Van Aken AFJ, Schnee M, Jörs S, Kros CJ, Ricci AJ & Heller S (2007). A helix-breaking mutation in TRPML3 leads to constitutive activity underlying deafness in the varitint-waddler mouse. *Proc Natl Acad Sci U S A* **104**, 19583–19588.

Helyer RJ, Kennedy HJ, Davies D, Holley MC & Kros CJ (2005). Development of outward potassium currents in inner and outer hair cells from the embryonic mouse cochlea. *Audiol Neurootol* **10**, 22–34.

Johnson KR, Zheng QY, Weston MD, Ptacek LJ & Noben-Trauth K (2005). The *Mass1*^{frings} mutation underlies early onset hearing impairment in BUB/BnJ mice, a model for the auditory pathology of Usher syndrome IIC. *Genomics* **85**, 582–590.

Kim HJ, Jackson T & Noben-Trauth K (2002). Genetic analyses of the mouse deafness mutations varitint-waddler (Va) and jerker (Espnje). *J Assoc Res Otolaryngol* **4**, 83–90.

Kim HJ, Li Q, Tjon-Kon-Sang S, So I, Kiselyov K & Muallem S (2007). Gain-of-function mutation in TRPML3 causes the mouse varitint-waddler phenotype. *J Biol Chem* **282**, 36138–36142.

Kim HJ, Li Q, Tjon-Kon-Sang S, So I, Kiselyov K, Soyombo AA & Muallem S (2008). A novel mode of TRPML3 regulation by extracytosolic pH absent in the varitint-waddler phenotype. *EMBO J* **27**, 1197–1205.

Kros CJ, Rüsch A, Lennan GWT & Richardson GP (1993). Voltage dependence of transducer currents in outer hair cells of neonatal mice. In *Biophysics of Hair Cell Sensory Systems*, ed. Duifhuis H, Horst JW, van Dijk P & van Netten SM, pp. 141–150. World Scientific, Singapore.

Kros CJ, Rusch A & Richardson GP (1992). Mechano-electrical transducer currents in hair cells of the cultured neonatal mouse cochlea. *Proc Biol Sci* **249**, 185–193.

Küssel-Andermann P, El-Amraoui A, Safieddine S, Nouaille S, Perfettini I, Lecuit M, Cossart P, Wolfrum U & Petit C (2000). Vezatin, a novel transmembrane protein, bridges myosin VIIA to the cadherin-catenins complex. *EMBO J* **19**, 6020–6029.

Lumpkin EA & Hudspeth AJ (1995). Detection of Ca^{2+} entry through mechanosensitive channels localizes the site of mechanoelectrical transduction in hair cells. *Proc Natl Acad Sci U S A* **92**, 10297–10301.

McGee J, Goodyear RJ, McMillan DR, Stauffer EA, Holt JR, Locke KG, Birch DG, Legan PK, White PC, Walsh EJ & Richardson GP (2006). The very large G-protein-coupled receptor VLGR1: a component of the ankle link complex required for the normal development of auditory hair bundles. *J Neurosci* **26**, 6543–6553.

Manzoni M, Monti E, Bresciani R, Bozzato A, Barlati S, Bassi MT & Borsani G (2004). Overexpression of wild-type and mutant mucolipin proteins in mammalian cells: effects on the late endocytic compartment organization. *FEBS Lett* **567**, 219–224.

Marcotti W & Kros CJ (1999). Developmental expression of the potassium current $I_{K,n}$ contributes to maturation of mouse outer hair cells. *J Physiol* **520**, 653–660.

Marcotti W, van Netten SM & Kros CJ (2005). The aminoglycoside antibiotic dihydrostreptomycin rapidly enters mouse outer hair cells through the mechano-electrical transducer channels. *J Physiol* **567**, 505–521.

Meyers JR, MacDonald RB, Duggan A, Lenzi D, Standaert DG, Corwin JT & Corey DP (2003). Lighting up the senses: FM1-43 loading of sensory cells through nonselective ion channels. *J Neurosci* **23**, 4054–4065.

Michalski N, Michel V, Bahloul A, Lefèvre G, Barral J, Yagi H, Chardenoux S, Weil D, Martin P, Hardelin JP, Sato M & Petit C (2007). Molecular characterization of the ankle-link complex in cochlear hair cells and its role in the hair bundle functioning. *J Neurosci* **27**, 6478–6488.

Nagata K, Zheng L, Madathany T, Castiglioni AJ, Bartles JR & Garcia-Anoveros J (2008). The varitint-waddler (Va) deafness mutation in TRPML3 generates constitutive, inward rectifying currents and causes cell degeneration. *Proc Natl Acad Sci U S A* **105**, 353–358.

Pataky F, Pironkova R & Hudspeth AJ (2004). Radixin is a constituent of stereocilia in hair cells. *Proc Natl Acad Sci U S A* **101**, 2601–2606.

Pedersen SF, Owsianik G & Nilius B (2005). TRP channels: an overview. *Cell Calcium* **38**, 233–252.

Qian F & Noben-Trauth K (2005). Cellular and molecular function of mucolipins (TRPML) and polycystin 2 (TRPP2). *Pflugers Arch* **451**, 277–285.

Ricci AJ & Fettiplace R (1997). The effects of calcium buffering and cyclic AMP on mechano-electrical transduction in turtle auditory hair cells. *J Physiol* **501**, 111–124.

Ricci AJ, Kachar B, Gale J & Van Netten SM (2006). Mechano-electrical transduction: New insights into old ideas. *J Membr Biol* **209**, 71–88.

Russell IJ & Richardson GP (1987). The morphology and physiology of hair cells in organotypic cultures of the mouse cochlea. *Hear Res* **31**, 9–24.

Szegezdi E, Logue SE, Gorman AM & Samali A (2006). Mediators of endoplasmic reticulum stress-induced apoptosis. *EMBO Rep* **7**, 880–885.

Venkatachalam K, Hofmann T & Montell C (2006). Lysosomal localization of TRPML3 depends on TRPML2 and the mucolipidosis-associated protein TRPML1. *J Biol Chem* **281**, 17517–17527.

Waguespack J, Salles FT, Kachar B & Ricci AJ (2007). Stepwise morphological and functional maturation of mechanotransduction in rat outer hair cells. *J Neurosci* **27**, 13890–13902.

Xu H, Delling M, Li L, Dong X & Clapham DE (2007). Activating mutation in a mucolipin transient receptor potential channel leads to melanocyte loss in varitint waddler mice. *Proc Natl Acad Sci U S A* **104**, 18321–18326.

Acknowledgements

This work was supported by EuroHear, an EU Integrated Project (C.J.K. and G.P.R.), an MRC Programme Grant (C.J.K.), the Division of Intramural Research at NIDCD (K.N.-T.) and a Wellcome Trust grant (G.P.R.). W.M. is a Royal Society University Research Fellow. We thank Kuni Iwasa and Susan Sullivan for comments on earlier versions of this manuscript.

Author's present address

W. Marcotti: Department of Biomedical Science, University of Sheffield, Western Bank, Sheffield S10 2TN, UK.